HHS Public Access

Author manuscript

Arch Oral Biol. Author manuscript; available in PMC 2017 March 01.

Published in final edited form as:

Arch Oral Biol. 2016 March ; 63: 82–92. doi:10.1016/j.archoralbio.2015.11.021.

Effect of proteoglycans at interfaces as related to location, architecture, and mechanical cues

Michael P. Kurylo[a], **Kathryn Grandfield**[a], **Grayson W. Marshall**[a], **Virginia Altoe**[b], **Shaul Aloni**[b], and **Sunita P. Ho**[a,*]

[a]Division of Biomaterials and Bioengineering, Department of Preventive and Restorative Dental Sciences, School of Dentistry, University of California, San Francisco, San Francisco, CA 94143, United States

[b]Materials Division, The Molecular Foundry, Lawrence Berkeley National Laboratory, Berkeley, CA, United States

Abstract

Introduction—Covalently bound functional GAGs orchestrate tissue mechanics through time-dependent characteristics.

Objective—The role of specific glycosaminoglycans (GAGs) at the ligament–cementum and cementum–dentin interfaces within a human periodontal complex were examined. Matrix swelling and resistance to compression under health and modeled diseased states was investigated.

Materials and methods—The presence of keratin sulfate (KS) and chondroitin sulfate (CS) GAGs at the ligament–cementum and cementum–dentin interfaces in human molars ($N = 5$) was illustrated by using enzymes, atomic force microscopy (AFM), and AFM-based nanoindentation. The change in physical characteristics of modeled diseased states through sequential digestion of keratin sulfate (KS) and chondroitin sulfate (CS) GAGs was investigated. One-way ANOVA tests with $P < 0.05$ were performed to determine significant differences between groups. Additionally, the presence of mineral within the seemingly hygroscopic interfaces was investigated using transmission electron microscopy.

Results—Immunohistochemistry ($N = 3$) indicated presence of biglycan and fibromodulin small leucine rich proteoglycans at the interfaces. Digestion of matrices with enzymes confirmed the presence of KS and CS GAGs at the interfaces by illustrating a change in tissue architecture and mechanics. A significant increase in height (nm), decrease in elastic modulus (GPa), and tissue deformation rate (nm/s) of the PDL-C attachment site (215 ± 63–424 ± 94 nm; 1.5 ± 0.7–0.4 ± 0.2 GPa; 21 ±7–48 ± 22 nm/s), and cementum–dentin interface (122 ± 69–360 ± 159 nm; 2.9 ±1.3–0.7 ±0.3 GPa; 18 ± 4–30 ± 6 nm/s) was observed.

*Corresponding author. Sunita.ho@ucsf.edu (S.P. Ho).

Conflict of interest

The authors have no conflict of interest to declare.

Ethical approval

Ethical approval was provided by the UCSF Committee on Human Research.

Conclusions—The sequential removal of GAGs indicated loss in intricate structural hierarchy of hygroscopic interfaces. From a mechanics perspective, GAGs provide tissue recovery/resilience. The results of this study provide insights into the role of GAGs toward conserved tooth movement in the socket in response to mechanical loads, and modulation of potentially deleterious strain at tissue interfaces.

Keywords

Interfaces; Glycosaminoglycans; Tissue recovery; Tissue mechanics; Indentation

1. Introduction

In load bearing organs, several structural elements interact at various hierarchical length-scales. Interactions over length scales include microscale structural elements within cells that interface with matrix proteins through connective networks, which in turn maintain macroscale organ function. However, within this broad classification, there exists the need for a finer discretization to investigate the interplay of two dominant and distinctly shaped structural elements; fibrillar collagen and nonfibrillar proteoglycans (PGs). PGs interact with collagen and maintain mechanical and structural integrity of tissues (Ho, Sulyanto, Marshall, & Marshall, 2005), specifically at the attachment site of soft and hard tissues of a load bearing organ such as the dentoalveolar complex.

PGs act as macro-molecular struts between collagen fibrils and provide time-dependent characteristics identified as a shape memory property of tissues and their interfaces. Load-dampening characteristics of softer tissues are also maintained by the molecular integrity within collagen fibrils and covalently bonded PGs. When chemically bound, the two structurally and chemically different macromolecules provide load-dampening and tissue resilience characteristics. Resilience is often indicated by the ability of tissues to recover in size and shape over time upon load removal, and provides the tissue with shape memory. The time-dependent response to load is the viscous behavior of tissues. In the bone–ligament–tooth fibrous joint, the ligament is biphasic as it is a combination of fluid and solid phases. The fluid-like properties aid in lubrication, nutrient delivery, and hydrostatic pressure, all of which maintain organ vitality, and the ability of PDL to dampen dynamic loads. At healthy attachment sites, cohesive and adhesive bonds between structurally dissimilar macromolecules remain intact despite concentration differences, and natural turnover of different molecules. However, intact bonds between structural elements do not prevail under diseased or chronic inflammatory conditions (Embery, Waddington, Hall, & Last, 2000), and this in turn could change the time related response of tissues to mechanical loads. Thus, there lies the need to understand the effect of deteriorated PGs on organ function, specifically at the earlier stages of deterioration.

Higher and lower molecular weight PGs also known as non-aggregating and aggregating types form covalent bonds with collagen (Seog et al., 2002). These macromolecules are thought to be key players in absorbing dynamic mechanical loads, specifically within the collagen-rich soft tissue and at attachment sites that are an integral part of an organ. Within these tissues that predominantly contain type I collagen, the higher molecular weight PGs retain hydrostatic pressure and gross shape characteristics (Seog et al., 2002 Scott, 1988;

Scott & Haigh, 1988), while lower molecular weight PGs within the same tissues and their adjacent interfaces are thought to maintain site-specific biophysical and biochemical environment for cells. Site-specific activities for cells promote and maintain local levels of organic and inorganic ratios at the ligament–bone and ligament–cementum attachment sites. In the human periodontium, the local levels of organic to inorganic components are predominantly reflected in precementum and osteoid layers relative to the respective bulk tissues that form the bone–PDL–tooth complex.

In the human periodontal complex, the prevalent PG families are of a lower molecular weight and belong to a family known as the small leucine rich proteoglycans (SLRPs). The protein cores of SLRPs have a mass between 45 and 55 kDa, leucine-rich repeats (LRRs) and typically contain covalently bound functional glycosaminoglycans (GAGs). Although the protein core of SLRPs binds directly to collagen, it is the associated GAGs that orchestrate several tissue characteristics including fibrillogenesis, spacing of the fibrils, and subsequent mineralization, thus modulating overall tissue mechanics (Scott, 1988). PGs have been identified within mineralized tissues as well as the mineral-free periodontal ligament (PDL) (Ababneh, Hall, & Embery, 1998; Ababneh, Hall, & Embery, 1999; Ho, Marshall, Ryder, & Marshall, 2007; Matheson, Larjava, & Hakkinen, 2005). PGs were also identified at the PDL–bone, PDL–cementum interfaces (Ho et al., 2010; Hurng et al., 2011; Lukinmaa, Mackie, & Thesleff, 1991). Previous studies from our laboratory have identified hygroscopic regions of the PDL–bone, PDL–cementum interfaces alluding to the presence of SLRPs (Ho et al., 2010; Hurng et al., 2011) and subsequently have identified SLRPs at the attachments sites (Chiu et al., 2012). Additionally, the presence of chondroitin sulfated GAGs was confirmed at a similar region, but at an interface between mineralized tissues, cementum and dentin within the complex of human molars (Ho, Balooch et al., 2004) (Yamamoto et al., 1999). Chondroitin-sulfated GAGs were also thought to be responsible for retaining radial fibrillar structure and mechanical properties of interfaces (Ho et al., 2005; Scott, 1988; Scott and Haigh, 1988; Scott and Stockwell, 2006; Yamamoto et al., 1999; Yamamoto, Domon, Takahashi, Islam, & Suzuki, 2000). In this study, we present two specific anatomical locations within a tooth that continue to be hypothesized as strain amplification sites (Qian, Todo, Morita, Matsushita, & Koyano, 2009; Ho et al., 2013). These include, (1) attachment sites (entheses) and interfacial zones where the pure organic PDL changes to mineralized cementum through PDL-inserts (also known as Sharpey's fibers) held together by cementum layer; (2) the cementum–dentin interface which was described as PDL-inserts attaching with root dentin forming a hygroscopic region commonly known as the CDJ (Ho, Balooch et al., 2004). A conceivable challenge to address the objective is the accessibility of attachment sites and the relevance of site-specific physical properties within the context of organ mechanics. In this study, the aforementioned challenge will be addressed through a commonly sought reductionist approach. The approach will include isolation of specific regions of interest in order to investigate the loss in tissue recovery characteristic due to breakdown of macromolecular tags, the PGs, and results will be discussed within the context of organ function. Thus, the objectives of this study are to investigate the crucial influence of GAGs, especially keratan sulfate and chondroitin sulfate at the PDL–cementum and cementum–dentin interfaces including cementum and dentin of the bone–ligament–tooth fibrous joint. Although a few studies have

proposed CS containing SLRPs and high molecular weight PGs (such as lumican, versican, aggrecan, etc.) resist compressive and shear forces (Ho et al., 2007; Scott and Stockwell, 2006), little to no information about the overall mechanical influence of these biochemical moieties that aid in tissue recovery nature exists.

2. Materials and methods

2.1. Specimen preparation for immunohistochemistry

Extracted molars (N = 3) were coarsely sectioned and fixed in sodium phosphate-buffered (pH 7.0) 4% formaldehyde for 3 days. Specimens were demineralized using immunocal (Decal Chemical Corporation, Tallman, NY) formic acid solution for eight weeks, and were considered demineralized when addition of saturated ammonium oxalate to the solution failed to produce a precipitate.

2.1.1. Paraffin sections on microscope slides—Following dehydration with 80%, 95%, and 100% Flex alcohol (Richard-Allan Scientific, Kalamazoo, MI), the specimens were embedded in paraffin (Tissue Prep-II, Fisher Scientific, Fair Lawn, NJ). 5–6 μm thickness for histology sections was achieved with a rotary microtome (Reichert-Jung Biocut, Vienna, Austria) using disposable steel blades (TBF™ Inc., Shur/Sharp™, Fisher Scientific, Fair Lawn, NJ). The paraffin serial sections were mounted on Superfrost Plus microscope slides (Fisher Scientific, Fair Lawn, NJ).

2.1.2. Localizing KS- and CS-GAGs within the roots of human molars—Previously detailed (Ho et al., 2010) immunohistochemistry procedure was used to locate biglycan (BGN) and fibromodulin (FMOD) within cementum, the cementum dentin interface, and dentin. The respective antibodies for BGN and FMOD staining were obtained from Dr. Larry Fisher (NIDCR/NIH, Bethesda, MD), and are all polyclonal rabbit sera. Finally, 3,30-diaminobenzidine (DAB) enhanced liquid substrate system (Sigma, St. Louis, MO) was used per manufacturer's instructions with an incubation of 1 h to provide a brown coloration for epitope identification. An Olympus BX51 light microscope was used to characterize the slides using Image Pro software (Media Cybernetics Inc., Bethesda, MD).

2.2. Specimen preparation for light and atomic force microscopy techniques and site-specific indentation

Healthy molars (N = 5) were obtained from 18 to 30 year old human subjects requiring extractions as a part of dental treatment following a protocol approved by the UCSF Committee on Human Research. The teeth were sterilized using 0.31 Mrad of γ-radiation (Brauer, Saeki, Hilton, Marshall, & Marshall, 2008). The molars were sectioned using a diamond wafering blade and a low-speed saw (Isomet, Buehler, Lake Bluff, IL) under wet conditions. Each specimen yielded regions containing primary cementum, mid-root and apical blocks containing secondary cementum, and cementum–dentin interface and radicular cementum.

Each block was then glued to an AFM steel stub (Ted Pella, Inc., Redding, CA) using epoxy (ITW Devcon 5-min epoxy, Danvers, MA) for ultra-sectioning with an ultramicrotome. A diamond knife (MicroStar Technologies, Huntsville, TX) was used to perform final

sectioning by removing 300 nm thin sections permitting orthogonality between tip (nomial radius of curvature equal to 50 nm for AFM and 100 nm for nanoindentation) and the specimen; a necessary criterion for AFM and indentation (Ho, Goodis et al., 2004). The ultrasectioned blocks were characterized before and after GAG-digestion under dry and wet conditions using an AFM and an AFM-based nanoindenter.

2.2.1. Preparation of enzymes to digest lower and higher molecular weight GAGs—All protease-free enzymes were from Seikagaku Corporation Tokyo, Japan unless otherwise specified. Keratanase (KS, from Pseudomonas sp.) digested lower molecular weight KS-GAGs, and Chondroitinase-ABC (C-ABC, from Proteus vulgaris) has been shown to enzymatically cleave *N*-acetylhexosaminidase linkages of higher molecular weight GAG side chains of chondroitin sulfate (chondroitin-4-sulfate 'C4S,' chondroitin-6-sulfate 'C6S'), dermatan sulfate ('DS', often referred to as chondroitin sulfate B), and hyaluronic acid [3]. For the purpose of this study the specimens treated with chondroitinase-ABC will be collectively called 'CS' even though hyaluronan could have been affected. C-ABC does not act on keratan sulfate, heparin, or heparan sulfate (Scott and Haigh, 1988).

The lyophilized enzymes were diluted with 0.1% bovine serum albumin (BSA) (BP675-1, Fisher Scientific, Fair Lawn, NJ) to obtain a concentration of 0.1 IU/ml. All GAG-digestions were performed at a pH of 7.2 and a temperature of 37 °C. The diluted enzymes were stored in a −80 °C freezer to maintain enzyme efficacy and prevent denaturing. Upon each GAG digestion epoch, the specimen was gently rinsed with approximately 80 ml of 1X PBS (BP665-1, Fisher Scientific, Fair Lawn, NJ)

2.2.2. Time-related GAG-digestion studies—A pilot study to determine the time required to remove the KS-GAGs followed by CS-GAGs within detectable limits of instrumentation was first performed. Before GAG-digestion, topography data under dry and wet conditions was collected using an AFM. These baseline measurements were identified as the control group in this study. The first GAG-digestion was performed for one hour by immersing the ultramicrotomed specimens in approximately 130 μl of 0.1 IU/ml keratinase-enzyme solution at 37 °C; dry and wet AFM height data was collected post-digestion and was compared to the control. The specimens were then exposed to consequent 2-h sessions of KS-digestion and resulting topography data was collected until a plateau in topographical height was observed. C-ABC digestion for 7 h (Ho et al., 2005) was then performed on fully digested KS block specimens followed by final AFM scanning under dry and wet conditions.

2.3. Evaluation of structural changes using a contact mode atomic force microscope

The ultrasectioned blocks were initially imaged using a light microscope (BX 51, Olympus America Inc., San Diego, CA) to identify primary and secondary cementum types. Quantitative structural analyses of the undigested (control) and GAG-digested ultrasectioned specimens under dry and wet conditions were conducted using a contact mode AFM (Nanoscope III, Multimode; DI-Veeco Instruments Inc., Santa Barbara, CA) with a 'J' type piezo scanner at a frequency of 1.6 Hz. A Si_3N_4 tip attached to a "V shaped" type 'D' cantilever, with a nominal normal spring constant of 0.03 Nm^{-1} (DI-Veeco Instruments Inc.,

Santa Barbara, CA) and a nominal radius of curvature less than 50 nm, was used to scan the specimens.

Five cementum-dentin interface sites, maximum scan size of 140 μm × 140 μm, and five cementum sites containing PDL-inserts in cementum with a maximum scan size of 80 μm × 80 μm, were examined at both dry and wet conditions. Tissue swelling was calculated by averaging the height of the region of interest. Care was taken to keep the scan sites the same between the controls, KS-GAG digested, and KS + CS-GAG digested specimens. Finally, the heights of the interfaces binding primary cementum to dentin (PC-CDJ), and secondary cementum to dentin (SC–CDJ) were recorded and analyzed. Average height for PC–CDJ, SC–CDJ, and PDL-inserts through SC was compared. ANOVA statistical analysis was performed to evaluate significant differences across each tissue type at different digestion time points.

2.4. Transmission electron microscopy (TEM) of ultrathin sections

90 nm ultrathin sections corresponding to the surface studied by AFM, were coated with a thin (~5 nm) layer of carbon and analyzed in a JEOL 2100F Field Emission TEM operated at 120 keV. Conventional bright-field TEM image of the cementum–dentin interface was recorded. The texture of collagen within the cementum–dentin interface was analyzed with selected-area electron diffraction (SAED) patterns.

2.5. Evaluation of site-specific mechanical response using AFM-based nanoindentation

Nanomechanical tests on hydrated specimens ($N = 5$) were performed using an AFM-based nanoindenter. Immersion of the specimen and indenter in distilled water for a minimum of 1 h closely mimicked *in vivo* conditions. A sharp diamond Berkovich indenter with a radius of curvature less than 100 nm (Triboscope Micromechanical Test Instrument, Hysitron Incorporated, MN) was fitted to a load-displacement transducer (Triboscope Micro-mechanical Test Instrument, Hysitron Incorporated, Minneapolis, MN). The site specificity for indentation was maintained by using an nPoint piezo scanner (nPoint Inc., Middleton, WI, USA) on the AFM.

For each tissue type within a single block (dentin, cementum–dentin interface, cementum, and PDL-inserts) a minimum of 30 indents were made over 3 different scan areas (50 μm × 50 μm scans) distributed across the entire length of the block. Data was collected for the control, KS-digested, and KS + CS-digested time points. Under the closed-looped load setting provided by the data acquisition software (Triboscope Micromechanical Test Instrument, Hysitron Incorporated, Minneapolis, MN) a force of 1000 μN was applied in a load, hold, and unload pattern with each segment for 3 s. The unloading segment of the force-depth curve was analyzed to determine the reduced elastic modulus ‘Er’ of each indent. Furthermore, the tissue response during the hold portion was used to determine the change in deformation rate as GAGs were removed. Fused silica was used as a calibration standard for the AFM-nanoindenter.

3. Results

3.1. Mapping of biglycan and fibromodulin

Biglycan and fibromodulin were identified through antibody tagging of respective core proteins. Positive staining for both PGs within primary and secondary cementum (not shown) was observed and not just limited to circumferential-PDL (Fig. 1A, B), PDL-inserts in cementum (Fig. 1A and B; asterisks), and cementum–dentin interface (Fig. 1C).

A consistent positive stain was identified in the PDL-inserts (Fig. 1A and B; between solid arrows) as they transitioned from the higher concentration in the PDL-space into the mineralized cementum. Although not consistent, lamellar layers within SC stained for biglycan and fibromodulin. Complementing the PDL-insert staining, a pronounced and highly concentrated stain was observed at the cementum–dentin interface (Fig. 1C) for both PGs. Fig. 1D illustrates the negative control specimen.

3.2. Structural influences of GAGs on PDL-inserts, secondary cementum lamellae, and the cementum–dentin interface

3.2.1. Swelling is indicated by an increase in topographical height: enthesis, PDL-inserts, cementum–dentin interface—Fig. 2 illustrates higher resolution AFM images under wet conditions of an ultrasectioned block. Specific regions B and C are shown at a higher resolution. Fig. 2B illustrates swollen PDL-inserts, while Fig. 2C illustrates a swollen cementum–dentin interface. By analyzing the same site before and after GAG-digestion as seen in Fig. 3, digestion of GAGs increased the confidence in detecting changes in tissue structure.

Fig. 3 illustrates the change in heights of cementum and near the attachment site (Fig. 3A–C), PDL-inserts (Fig. 3A–C; asterisk), SC, and the cementum-dentin interface (Fig. 3D–F) upon sequential removal of KS and then CS GAG moieties. Qualitatively, PDL-inserts within cementum and those attaching to dentin at the cementum–dentin interface had the most pronounced swelling identified as an increase in height compared to the surrounding tissue. Although the entire cementum–dentin interface region (Figs. 2 C and 3 D–F) was characterized by significant swelling, the PDL-inserts within the cementum–dentin interface had the greatest amount of controlled swelling and increased upon GAG removal. It was noted that the hypomineralized attachment sites lost structural integrity upon GAG digestion and were distinguishable from the highly mineralized cementum (Ho et al., 2010).

The average height of the PC–CDJ and SC–CDJ and PDL-inserts are also presented in Fig. 3. ANOVA analysis revealed significant differences ($P < 0.05$) across all digestion time points for each analyzed tissue. Interestingly, undigested SC–CDJ (control) had significantly more swelling compared to undigested PC (control). Moreover, except for complete KS + CS removal, SC–CDJ and PDL height were very similar for each condition measured.

Complete GAG digestion was determined based on a plateau in cementum–dentin interface and PDL-insert heights under hydrated conditions. A steady increase in swelling from the initial baseline measurements from control specimens was seen after total digestion times of 1, 3, and 5 h with the keratinase. After 7 h digestion the height of both tissue types did not

depart from the recorded heights from the 5-h digestion; a 9-h long digestion further confirmed no change in height. Similar procedures were performed with chondroitinase-ABC on the KS-digested blocks; similar results were obtained, but showed a more pronounced effect after one hour digestion with C-ABC, after which no additional change was observed.

3.2.2. Loss of structural integrity with removal of GAGs: Dry AFM scans—Dry AFM micrographs of controls (Fig. 4A) revealed minimal height variation across all tissue types. However, upon KS digestion of the PC–CDJ (Fig. 4B) and SC–CDJ (not shown) a valley was formed. Increased digestion time caused more removal of KS + CS GAGs (Fig. 4C) making the valley deeper and delineating cementum from dentin. An increasing trend was observed until digestion time was equal to 7 h. At 7 h and beyond, no more changes in depth of the valley were detected by using the AFM under wet or dry conditions. Interestingly, the formation of a lamellar pattern often a characteristic of SC was also observed in PC after digestion of GAGS. Higher resolution scans (Fig. 4D and E) revealed a repeated banding pattern of valleys and peaks spaced around 300–500 nm with a height variation of ~200 nm (Fig. 4). The layered appearance was observed over the bulk primary cementum. Removal of KS and CS complexes within dry scans of SC enhanced the characteristic lamellar pattern.

3.3. Texture of the cementum–dentin interface

A bright-field (BF) image with insets of selected area electron diffraction (SAED) patterns at regions from 1 to 3 is marked in Fig. 5. Corresponding dark-field (DF) images highlight the orientation of hydroxyapatite crystals along the 002 *c*-axis, which coincides with collagen fibril direction indicating the presence of intrafibrillar mineral. While crystal orientation maintains a close match to fibril direction, SAED and DF indicate a spread in crystal orientation within the regions sampled and a strong possibility of the presence of extra-fibrillar mineral.

3.4. Mechanical response of the PDL-inserts, PC, SC and cementum–dentin interface with and without GAGs

Averaged results for the elastic modulus and tissue deformation rate are detailed in Fig. 6. Elastic modulus values for controls initially revealed that both SC–CDJ and SC-bulk cementum (labelled as CEM) have a slightly higher resistance to mechanical loads than PC–CDJ and PC. Additionally, PDL-inserts through SC had the lowest elastic modulus. Upon removing KS, a 50% decrease in elastic modulus was observed within all regions. Interestingly, the inherent modulus differences between PC-CEM and SC-CEM, PC–CDJ and SC–CDJ were completely removed upon KS digestion resulting in similar responses to indentation loads. The loss of KS also resulted in a greater tissue deformation rate for PDL-inserts and the CDJ as seen in an extension of region B of Fig. 5. It was also noted that although dentin was not positively stained for KS and CS in Fig. 1 a drastic drop in its elastic modulus was observed; a significant difference between the two dentin types interfacing the two cementum types was observed. Removal of CS moieties resulted in similar trends with a decrease in elastic modulus and a significant increase in tissue

deformation. ANOVA tests revealed a significant decrease in elastic modulus and tissue deformation ($P < 0.05$) across all digestion time points for each tissue.

4. Discussion

The bone–ligament–tooth complex has four mineralized tissues of differing stiffness values and tissue resilience. The enamel (harder tissue), dentin and cementum of the tooth are connected to alveolar bone of the jaw by the way of cementum via a viscous and load dampening PDL. The novel aspect of this study on the complex involves highlighting the spatial distribution of load dampening molecules at site-specific regions of the PDL–cementum enthesis and the cementum–dentin interface. Molecules include biglycan and fibromodulin containing higher and lower molecular weight CS- and KS-GAGs, which interconnect with collagen. These interconnecting elements are postulated to maintain needed tissue resilience for conserved tooth movement within the alveolar socket.

Identification of biglycan and fibromodulin PGs was performed through immunohistochemistry, selective digestion of KS- and CS-GAGs, followed by site-specific probing to evaluate changes in tissues' architecture and response to mechanical loads. Rate of tissue deformation to mechanical loads was investigated to understand the multi-dimensional functionality at entheses and interfaces that in turn are known to affect organ biomechanics. Examples of entheses in the articulating musculoskeletal joints include, the ligament–bone and tendon–bone fibrocartilaginous interfaces (Benjamin & McGonagle, 2009). Within the oral and craniofacial systems, the ligament-alveolar bone and ligament–cementum fibrous interfaces of the dentoalveolar fibrous joint (Ho et al., 2010; Hurng et al., 2011; McCulloch, Lekic, & McKee, 2000) are responsible in part for the overall mechanics of fibrous joints. Because of the mismatch in elasticity at the ligament–cementum and cementum–dentin interfaces, from a pure engineering perspective strain concentrations should exist at the attachment sites and interfaces within load bearing joints (Ho et al., 2013; Qian et al., 2009). However, results from this study using higher resolution site-specific microscopy and indentation illustrate otherwise. Our results highlighted an abundance of adhesive molecules at the PDL–cementum and cementum–dentin interfaces. Breakdown of PGs by using enzymes provided insights into the maintenance of collagen orientation and thereby the strain-dampening characteristics of interfaces. The innate polyanionic nature of GAGs is pivotal in maintaining free-charge density, electrostatic interactions, steric hindrance, water retention, hydrostatic pressure, lubrication, nutrient transport, cell migration, cell differentiation, matrix structure, and mechanical integrity (Seog et al., 2002) all of which are necessary to conserve the biomechanical integrity of the bone–ligament–tooth complex. These results highlight the presence of GAGs to be axiomatic. From a mechanics perspective the presence of GAGs provides tissue resilience, and consequently a conserved tooth movement in the socket occurs as a response to functional loads. However, it is likely that strain concentrations owing to material mismatch can occur if pathological levels of strain exist, that is, beyond physiological threshold limits shifting the homeostasis of the interface to a diseased state (a significant shift in GAG concentration) causing enthesopathies (Benjamin et al., 2004). For functional attachment of dissimilar harder materials such as cementum (2.5–5.5 GPa) with dentin (14.0–21 GPa), it is interesting to note that the hygroscopicity of the cementum–dentin interface decreased with an increase in

age (Jang et al., 2014), and perhaps cementum fusing with dentin can increase the risk for tooth fracture with age.

Based on previous results, a healthy dentoalveolar fibrous joint does not provide a discrete or an abrupt transition in mechanical properties from PDL to cementum, and cementum to dentin. The measured elastic gradients across these interfaces (Ho, Balooch et al., 2004; Ho et al., 2009; Lin et al., 2013) could also be due to significant dependence and communication between concentration gradients of biomolecules and in particular GAGs within the softer periodontal ligament and harder cementum, and dentin and cementum tissues to mediate and adapt to function-related stresses and strains. Hence, ligament–cementum enthesial sites, and cementum–dentin interfaces are exceptional “models” for examining the role of PGs and their critical role in developing/regenerating osteoid-like and cementum-like tissues.

The intermediate cementum-like and osteoid-like tissues contain higher ratios of organic to inorganic due to the presence of GAGs, a subunit of PGs. The two interfaces interrogated in this study were PG-rich (Fig. 1), and demonstrated (1) loss in fibrillar structure in the predominantly hygroscopic regions of the PDL-cementum and cementum-dentin interfaces where higher concentrations of the PGs were identified (Figs. 2 and 3); (2) visualization of finer lamellae within primary cementum (revealing structures that were thought not to exist) (Fig. 4); (3) a significant increase in rate of tissue deformation upon digestion of the lower molecular weight GAGs followed by higher molecular weight GAGs demonstrating the importance of a molecular weight in overall retention of tissue resilience. By performing microscopy on the same regions under dry and wet conditions, we were able to highlight organic regions. As described in our previous work (Ho et al., 2005), the collagenous matrix could collapse in regions of higher ratios of organic to inorganic (Fig. 3 in Ho et al., 2005). However, under wet conditions, the attraction of water molecules by the GAGs within the collagen-PG network transformed the valley into a peak similar to the absorption of water by a dry sponge. In this study, the transformation from valley to a peak was termed as swelling (Ho et al., 2005). Immunolocalization of higher concentration of GAGs (Fig. 1) which could either be a part of non-aggregating (including aggrecan, and versican) and/or aggregating molecules (including lumican, fibromodulin, decorin, and biglycan) caused swelling of the organic-dominant regions at the enthesis and cementum–dentin interface (Figs. 2 and 3). In our previous study (Ho et al., 2005) we demonstrated that GAGs in the cementum–dentin interface retain structure and alluded that their retention could provide shape memory to tissues. A similar concept about GAGs, but as modulators of shape and architecture was put forth by Scott and Thomlinson (1998) and was related to extracellular matrix of fibrous connective tissues (Scott and Thomlinson, 1998).

Retention of matrix integrity both in shape and mechanical properties is essential for tissue recovery. In order to investigate the effect of GAGs on the structure and mechanical recovery of tissues/interfaces, changes in structure and mechanical properties were mapped following sequential digestion of lower followed by higher molecular weight GAGs. From a structural perspective, a loss in fibrillar structure in the predominantly hygroscopic regions of the PDL-cementum and cementum-dentin interface was observed. These results (Fig. 3) highlighted the importance of GAGs as molecular tacks for collagen fibrils. Assuming that

GAGs exist all over within mineralized tissues and soft tissues, results illustrated significant changes in organic dominant regions. The digestion of molecular tacks causes' unconstrained motion of fibrillar structures specifically under wet conditions, and as a result is seen as an increase in height (increased deflection of AFM cantilever–a signal used to capture differences in topography) when scanning the enthesis and cementum–dentin interface under wet conditions. Swelling conditions as seen due to breakdown of CS- and KS-GAGs exist in periodontally diseased or mechanically impacted dentoalveolar complexes (Embery, Hall, Waddington, Septier, & Goldberg, 2001; Embery et al., 2000; Krishnan & Davidovitch, 2006; Krishnan & Davidovitch, 2009). Under these conditions, interestingly over time, the affected regions can have an altered pH, and free GAGs with an increased potential to collect ions including calcium and zinc causing concretion of cementum in the case of periodontitis, or forming woven bone, in the case of therapeutically displaced teeth. Hence, it is likely that under physiological conditions, despite the breakdown of PGs, mineral formation can occur however whether the formation is a favorable or a haphazard response could be dictated by extraneous signals that prompted GAG breakdown. Breakdown of extracellular network can also change porosity, permeability, interaction of ions in interstitial fluids, and fluid transport in response to load rates (Mow, Holmes, & Lai, 1984). These effects were highlighted elegantly by using articular cartilage (Wan, Miller, Guo, & Mow, 2004), and when performing biomechanics on an adapted bone–ligament–tooth fibrous joint (Lin, Lee, Özcoban, Schneider, & Ho, 2014).

In load bearing systems, the free charge density between GAGs, bound water, charge-based interactions with globular glycoproteins and fibrillar proteins, and steric hindrance between macromolecules promote an intrinsic strain in the extracellular matrix which is known as prestrain (Chen & Ingber, 1999). Prestrain in part contributes to the reactionary response of tissues when loaded. Resistance to load can also be affected by orientation and from sliding of fibrils until the resistance due to molecular bond strength between the fibril and the GAG is detected (Scott, 2001) as a reactionary force in response to tension, compression, and/or shear force. A fundamental example is fibronectin for which innate mechanical stretch in association with a GAG is necessary to expose the epitope, which in turn prompts events for matrix buildup. The intrinsic mechanical stretch can be translated to the mechanoresponsive nature of the forming matrix necessary for wound healing, or simply development of organic substrates on which stratified bone and cementum regenerate. This could be one of the reasons for observing the 250 nm lamellae in the primary cementum (Fig. 4) which to date has been reported as a cementum layer with a dominance of fibrous fringes. Evident within these examples is the self-healing nature of all natural systems, not simply due to the existence of a cell, but also due to the dynamic interplay between globular and fibrillar macromolecules.

Mechanoresponse due to dynamic interplay between macromolecules could exist at several different length scale levels. If so, could this be the reason why certain protein types are localized within regions that could be strain amplification sites, while lesser concentrations of GAGs and higher concentrations of mineral exist in stress dominated regions? The two key phrases in the aforementioned sentence are "localized within regions" and "strain amplification sites". Protein localization is evident at several regions highlighting the

making of a newer interface, a tissue regenerative region in response to innate matrix strain evident from changes in tissue recovery data (Fig. 6).

The intrinsic mechanoresponsive nature of a soft-hard tissue interface are highlighted by immunolocalization of water attracting glycosaminoglycans. The lower inorganic and higher organic content, and lower elastic modulus (Lin et al., 2013) can potentially serve as amorphous organic nuclei, or a medium conducive to inorganic mineral formation. At this juncture, it is necessary to state that the function of the organic nuclei can conceivably be a two-step model. This includes delivering calcium and other ions during and/or after fibril assembly, but before extrafibrillar binding of mineral forming ions, followed by fibril assembly to form mineralized tissues. However, this need not be true in organic regions, and could be limited to intrafibrillar mineralization as evidenced in the cementum–dentin interface. The effect of the observed tissue recovery is not limited to GAG tacks, and inorganic constituents can aid in tissue recovery as noted with percent tissue deformation for cementum–dentin interface relative to the enthesial region. This aspect was evident in our data that illustrated that percent tissue deformation for the enthesial region was higher compared to reinforced cementum–dentin interface regions. Enthesial regions are the GAG-dominant regions relative to cementum–dentin interface, and adjacent tissues cementum and dentin. However, based on pure hygroscopicity, it is interesting to note that both regions demonstrated similar hydration. A significant difference in tissue deformation by removing KS-GAGs was observed at all regions indicating that these regions could potentially contain fibromodulin and lumican of the SLRP family, and other types of KS-PGs including aggrecan. Changes in hydration, elastic modulus, and tissue response to load were also observed upon CS-GAG digestion. Based on significant differences due to removal of KS- and CS-GAGs respectively, results presented in this study are correlated with plausible immunolocalization of fibromodulin (KS-GAG) and biglycan (CS-, DS-GAG). In this study we digested KS first to investigate the effect due to lower molecular weight followed by digestion of higher molecular weight molecules under the assumption that higher molecular weight affect ECM more than lower molecular weight constituents. However results demonstrated that GAG concentration and presence is anatomy specific. The potential reasons for specificity could very well be that these regions are more dominant in SLRPs than nonaggregating molecules, and aid more in lubrication and retention of hydrostatic pressure within soft tissues.

The higher molecular weight GAGs exist in both aggregating proteoglycans and nonaggregating small leucine rich proteoglycans. Large aggregates such as aggrecan, versican, and hyaluronic acid are thought to provide hydrostatic pressure to tissues and as a result are responsible for resisting compressive loads. Hence, the function of aggregating molecules could be dominant at a larger length scale compared to a nonaggregating molecule. In our previous study we highlighted the mechanical characteristics of hygroscopic rich interface between two distinct mineralized tissues, cementum and dentin most evident in humans and the commonly sought mammalian models, the mouse and the rat. In this study, we highlighted their presence and tissue recovery characteristics at periodontal ligament (PDL)-cementum (soft-hard) interface taken from a human bone–ligament–tooth complex.

The results in this study are limited to anatomical specificity of PGs and their effect on tissue reaction to site-specific mechanical loads. However, it should be noted that the type of PG can be specific to an anatomical location, and that the site-specificity could be prompted by the overall biomechanics of the tooth articulating in the alveolar socket. The dynamic nature of the joint *per se* causes tension-dominated and compression-dominated regions within the organ which is thought to prompt different types and concentration of glycoproteins and affinities with inorganic constituents (Embery et al., 2000; Hurng et al., 2011; Kurylo, Nonomura, Marshall, Schuck, & Ho, 2011; Lin et al., 2013; McCulloch et al., 2000; Saffar, Lasfargues, & Cherruau, 1997). Along the same lines, it is plausible that different types of PGs could exist at these anatomical locations, which in turn aid in increasing or decreasing bioaffinities specific to mineral formation or resorption related events. Given the nature of the constituents at the attachment sites that include proteoglycans, collagen, glycoproteins, and bound water, it is important to note that a physical nature is necessary for cell migration, cell adhesion, cell proliferation, and differentiation all of which occur at the interface. Additionally, the interplay between macromolecules and interstitial fluid can be affected by varying input signals to the bone-tooth complex, i.e. therapeutic loads, and/or periodontal conditions. Other affecters include parafunction (bruxism and jaw clenching) that shift the organ to a pathologic state and potentially affect the type and concentration of PGs. In the absence of documentation on patients from whom the teeth were extracted and examined in this study, results highlight the presence of GAGs specific to large molecular weight CS, and lower molecular weight KS. As these GAGs can exist in a variety of PGs, the emphasis of the results is not on PGs *per se*, but that GAGs affect structure and mechanical integrity of tissues specifically at the PDL–cementum and cementum–dentin interfaces.

5. Conclusions

Immunolabelling provided the presence of biglycan and fibromodulin PGs. Digestion using enzymes indicated the role of high and low molecular weight GAGs, CS and KS, in the mechanical properties and structural organization at attachment sites of the human PDL–cementum and cementum–dentin interfaces. Site-specific examination of the structural changes arising from digestion of KS and CS indicated a loss in fibrillar structure in the predominantly hygroscopic regions of the PDL–cementum and cementum–dentin interfaces where higher concentrations of the PGs were identified. Similarly, a significant increase in rate of tissue deformation upon digestion of the lower molecular weight GAGs followed by higher molecular weight GAGs was noted, supporting the hypothesis that KS and CS contribute to the mechanical integrity of enthuses and attachment sites between dissimilar tissues in the dentoalveolar system. The data presented in this study provides insights to structural and mechanical conditions that could exist at the ligament–cementum enthesial site, and cementum–dentin junction under conditions of disease where loss of GAGs is prevalent.

Acknowledgments

The authors acknowledge funding support NIH/NIDCR R00DE018212 (SPH), NIH/NIDCR-R01DE022032 (SPH), NIH/NCRR S10RR026645, (SPH), Bioengineering & Biomaterials Micro-CT and Imaging Facility (http://bbct.ucsf.edu) and Departments of Preventive and Restorative Dental Sciences and Orofacial Sciences, UCSF;

Faculty of Engineering, McMaster University (Hamilton, Canada) (KG). The authors thank Dr. Marian Young (National Institutes of Dental and Craniofacial Research in Bethesda, MD), Prof. Marc McKee (McGill University in Montreal, Canada) and Prof. Arthur Veis (Northwestern University Feinberg School of Medicine, Chicago, IL) for technical discussions about proteoglycans and other matrix proteins, and their role in biomineralization. In addition, assistance from national facilities through user based program was provided by The Molecular Foundry, Lawrence Berkeley National Laboratory, Berkeley, CA. Work at the Molecular Foundry was supported by the Office of Science, Office of Basic Energy Sciences, of the U.S. Department of Energy under Contract No. DE-AC02-05CH11231.

References

Ababneh KT, Hall RC, Embery G. Immunolocalization of glycosaminoglycans in ageing, healthy and periodontally diseased human cementum. Archives of Oral Biology. 1998; 43:235–246. [PubMed: 9631176]

Ababneh KT, Hall RC, Embery G. The proteoglycans of human cementum: immunohistochemical localization in healthy, periodontally involved and ageing teeth. Journal of Periodontal Research. 1999; 34:87–96. [PubMed: 10207837]

Benjamin M, McGonagle D. Entheses: tendon and ligament attachment sites. Scandinavian Journal of Medicine & Science in Sports. 2009; 19:520–527. http://dx.doi.org/10.1111/j.1600-0838.2009.00906.x. [PubMed: 19522749]

Benjamin M, Moriggl B, Brenner E, Emery P, McGonagle D, Redman S. The enthesis organ concept: why enthesopathies may not present as focal insertional disorders. Arthritis & Rheumatology. 2004; 50:3306–3313. http://dx.doi.org/10.1002/art.20566.

Brauer DS, Saeki K, Hilton JF, Marshall GW, Marshall SJ. Effect of sterilization by gamma radiation on nano-mechanical properties of teeth. Dental Materials. 2008; 24:1137–1140. http://dx.doi.org/10.1016/j.dental.2008.02.016. [PubMed: 18436298]

Chen CS, Ingber DE. Tensegrity and mechanoregulation: from skeleton to cytoskeleton. Osteoarthritis and Cartilage. 1999; 7:81–94. http://dx.doi.org/10.1053/joca.1998.0164. [PubMed: 10367017]

Chiu R, Li W, Herber RP, Marshall SJ, Young M, Ho SP. Effects of biglycan on physico-chemical properties of ligament-mineralized tissue attachment sites. Archives of Oral Biology. 2012; 57:177–187. http://dx.doi.org/10.1016/j.archoralbio.2011.08.011. [PubMed: 21963335]

Embery G, Hall R, Waddington R, Septier D, Goldberg M. Proteoglycans in dentinogenesis. Critical Reviews in Oral Biology and Medicine. 2001; 12:331–349. [PubMed: 11603505]

Embery G, Waddington RJ, Hall RC, Last KS. Connective tissue elements as diagnostic aids in periodontology. Periodontology 2000. 2000; 24:193–214. [PubMed: 11276867]

Ho SP, Balooch M, Marshall SJ, Marshall GW. Local properties of a functionally graded interphase between cementum and dentin. Journal of Biomedical Materials Research. 2004; 70:480–489. http://dx.doi.org/10.1002/jbm.a.30105. [PubMed: 15293322]

Ho SP, Goodis H, Balooch M, Nonomura G, Marshall SJ, Marshall G. The effect of sample preparation technique on determination of structure and nanomechanical properties of human cementum hard tissue. Biomaterials. 2004; 25:4847–4857. http://dx.doi.org/10.1016/j.biomaterials.2003.11.047. [PubMed: 15120532]

Ho SP, Kurylo MP, Fong TK, Lee SSJ, Wagner HD, Ryder MI, et al. The biomechanical characteristics of the bone-periodontal ligament–cementum complex. Biomaterials. 2010; 31:6635–6646. http://dx.doi.org/10.1016/j.biomaterials.2010.05.024. [PubMed: 20541802]

Ho SP, Kurylo MP, Grandfield K, Hurng J, Herber RP, Ryder MI, et al. The plastic nature of the human bone–periodontal ligament–periodontal ligament–tooth fibrous joint. Bone. 2013; 57(2):455–467. http://dx.doi.org/10.1016/j.bone.2013.09.007. [PubMed: 24063947]

Ho SP, Marshall SJ, Ryder MI, Marshall GW. The tooth attachment mechanism defined by structure, chemical composition and mechanical properties of collagen fibers in the periodontium. Biomaterials. 2007; 28:5238–5245. http://dx.doi.org/10.1016/j.biomaterials.2007.08.031. [PubMed: 17870156]

Ho SP, Senkyrikova P, Marshall GW, Yun W, Wang Y, Karan K, et al. Structure, chemical composition and mechanical properties of coronal cementum in human deciduous molars. Dental Materials. 2009; 25:1195–1204. http://dx.doi.org/10.1016/j.dental.2009.04.005. [PubMed: 19464049]

Ho SP, Sulyanto RM, Marshall SJ, Marshall GW. The cementum–dentin junction also contains glycosaminoglycans and collagen fibrils. Journal of Structural Biology. 2005; 151:69–78. http://dx.doi.org/10.1016/j.jsb.2005.05.003. [PubMed: 15964205]

Hurng JM, Kurylo MP, Marshall GW, Webb SM, Ryder MI, Ho SP. Discontinuities in the human bone–PDL–cementum complex. Biomaterials. 2011; 32:7106–7117. http://dx.doi.org/10.1016/j.biomaterials.2011.06.021. [PubMed: 21774982]

Jang AT, Lin JD, Choi RM, Choi EM, Seto ML, Ryder MI, et al. Adaptive properties of human cementum and cementum dentin junction with age. Journal of the Mechanical Behavior of Biomedical Materials. 2014; 39C:184–196. http://dx.doi.org/10.1016/j.jmbbm.2014.07.015. [PubMed: 25133753]

Krishnan V, Davidovitch Z. Cellular, molecular, and tissue-level reactions to orthodontic force. American Journal of Orthodontics and Dentofacial Orthopedics. 2006; 129(469):e1–32. http://dx.doi.org/10.1016/j.ajodo.2005.10.007. [PubMed: 16627171]

Krishnan V, Davidovitch Z. On a path to unfolding the biological mechanisms of orthodontic tooth movement. Journal of Dental Research. 2009; 88:597–608. http://dx.doi.org/10.1177/0022034509338914. [PubMed: 19641146]

Kurylo MP, Nonomura G, Marshall GW, Schuck PJ, Ho SP. Localization and physico-chemical effects of glycosaminoglycans within molar interfaces. Presented at the 89th general session and exhibition of the IADR. 2011

Lin JD, Lee J, Özcoban H, Schneider GA, Ho SP. Biomechanical adaptation of the bone–periodontal ligament (PDL)–tooth fibrous joint as a consequence of disease. Journal of Biomechanics. 2014; 47:2102–2114. http://dx.doi.org/10.1016/j.jbiomech.2013.10.059. [PubMed: 24332618]

Lin JD, Özcoban H, Greene JP, Jang AT, Djomehri SI, Fahey KP, et al. Biomechanics of a bone–periodontal ligament–tooth fibrous joint. Journal of Biomechanics. 2013; 46:443–449. http://dx.doi.org/10.1016/j.jbiomech.2012.11.010. [PubMed: 23219279]

Lukinmaa PL, Mackie EJ, Thesleff I. Immunohistochemical localization of the matrix glycoproteins–tenascin and the ED-sequence-containing form of cellular fibronectin–in human permanent teeth and periodontal ligament. Journal of Dental Research. 1991; 70:19–26. [PubMed: 1704020]

Matheson S, Larjava H, Hakkinen L. Distinctive localization and function for lumican, fibromodulin and decorin to regulate collagen fibril organization in periodontal tissues. Journal of Periodontal Research. 2005; 40:312–324. http://dx.doi.org/10.1111/j.1600-0765.2005.00800.x. [PubMed: 15966909]

McCulloch CA, Lekic P, McKee MD. Role of physical forces in regulating the form and function of the periodontal ligament. Periodontology 2000. 2000; 24:56–72. [PubMed: 11276873]

Mow VC, Holmes MH, Lai WM. Fluid transport and mechanical properties of articular cartilage: a review. Journal of Biomechanics. 1984; 17:377–394. [PubMed: 6376512]

Qian L, Todo M, Morita Y, Matsushita Y, Koyano K. Deformation analysis of the periodontium considering the viscoelasticity of the periodontal ligament. Dental Materials. 2009; 25:1285–1292. http://dx.doi.org/10.1016/j.dental.2009.03.014. [PubMed: 19560807]

Saffar JL, Lasfargues JJ, Cherruau M. Alveolar bone and the alveolar process: the socket that is never stable. Periodontology 2000. 1997; 13:76–90. [PubMed: 9567924]

Scott JE. Proteoglycan–fibrillar collagen interactions. Biochemical Journal. 1988; 252:313. [PubMed: 3046606]

Scott JE. Structure and function in extracellular matrices depend on interactions between anionic glycosaminoglycans. Pathologie Biologie (Paris). 2001; 49:284–289. http://dx.doi.org/10.1016/s0369-8114(01)00152-3.

Scott JE, Haigh M. Identification of specific binding sites for keratan sulphate proteoglycans and chondroitin–dermatan sulphate proteoglycans on collagen fibrils in cornea by the use of cupromeronic blue in critical-electrolyte-concentration techniques. Biochemical Journal. 1988; 253:607–610. [PubMed: 2972275]

Scott JE, Stockwell RA. Cartilage elasticity resides in shape module decoran and aggrecan sumps of damping fluid: implications in osteoarthrosis. The Journal of Physiology (London). 2006; 574:643–650. http://dx.doi.org/10.1113/jphysiol.2006.108100. [PubMed: 16581860]

Scott JE, Thomlinson AM. The structure of interfibrillar proteoglycan bridges (shape modules') in extracellular matrix of fibrous connective tissues and their stability in various chemical environments. Journal of Anatomy. 1998; 192(Pt 3):391–405. [PubMed: 9688505]

Seog J, Dean D, Plaas AHK, Wong-Palms S, Grodzinsky AJ, Ortiz AC. Direct measurement of glycosaminoglycan intermolecular interactions via high-resolution force spectroscopy. Macromolecules. 2002; 35:5601–5615. http://dx.doi.org/10.1021/ma0121621.

Wan LQ, Miller C, Guo XE, Mow VC. Fixed electrical charges and mobile ions affect the measurable mechano-electrochemical properties of charged-hydrated biological tissues: the articular cartilage paradigm. Mechanics & Chemistry of Biosystems. 2004; 1:81–99. [PubMed: 16783948]

Yamamoto T, Domon T, Takahashi S, Islam H, Suzuki F, Wakita M. The structure and function of the cemento–dentinal junction in human teeth. Journal of Periodontal Research. 1999; 34:261–268. http://dx.doi.org/10.1111/j.1600-0765.1999.tb02252.x. [PubMed: 10567949]

Yamamoto T, Domon T, Takahashi S, Islam MN, Suzuki R. The fibrous structure of the cemento–dentinal junction in human molars shown by scanning electron microscopy combined with NaOH-maceration. Journal of Periodontal Research. 2000; 35:59–64. [PubMed: 10863959]

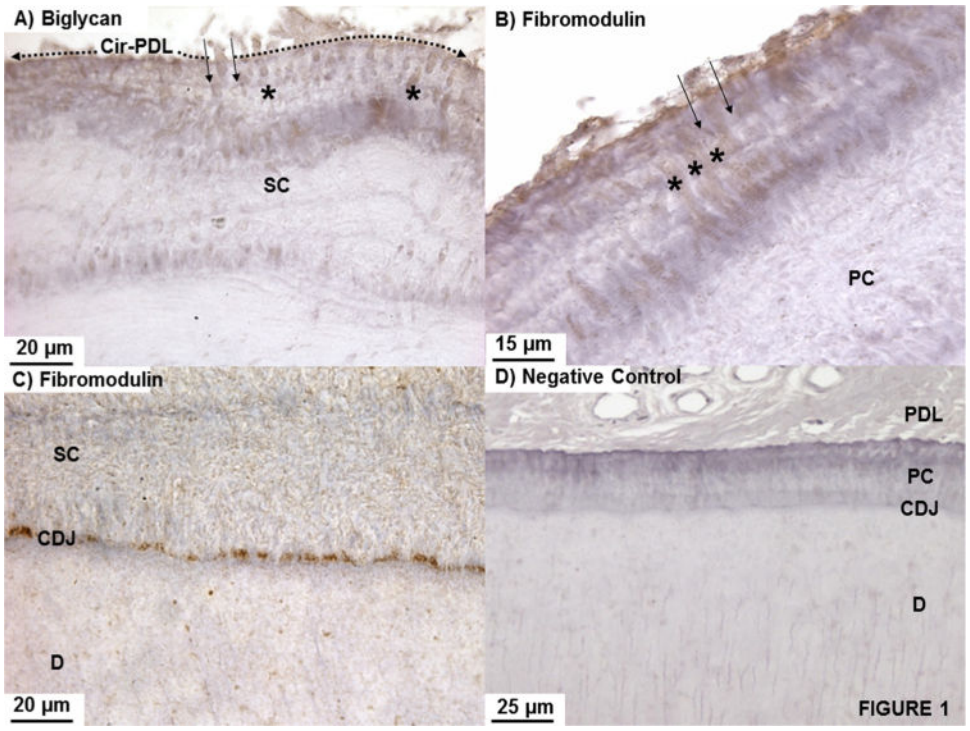

Fig. 1.

(A) Biglycan and (B) fibromodulin regardless of the type of cementum (secondary cementum-SC in (A); primary cementum–PC in (B)) were immunolocalized. PDL-inserts contained biglycan (between solid arrows) as it transitioned from the PDL-space into bulk cementum and coursed through cementum (asterisks) up to the CDJ (A–C). A negative control is shown in (D).

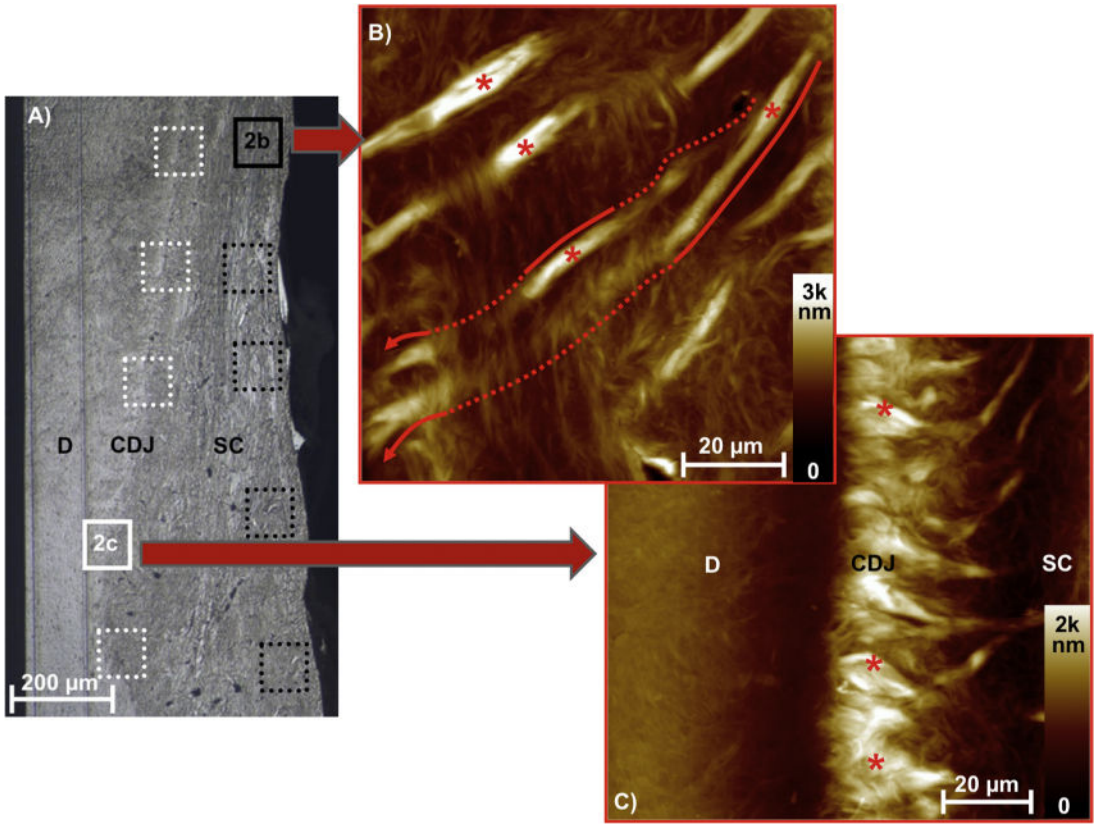

Fig. 2.

Light microscopy of a microtomed mid-root block (A) is shown with dentin—D, the cementum–dentin junction—CDJ, and secondary cementum—SC. Five regions within the CDJ (white boxes) and cementum (black boxes) were analyzed using AFM and AFM-based nanoindentation technique for each block. Intensity scale bars indicate topographical variation of organic dominant regions (visible PDL-inserts in B, and visible CDJ in C) under hydrated conditions. The PDL-inserts through cementum (B) meandered into (solid line) and out of (dashed line) the microtomed plane. Only the in-plane portions of PDL-inserts (asterisks) were analyzed to determine swelling as indicated by variation in topography and mechanical properties.

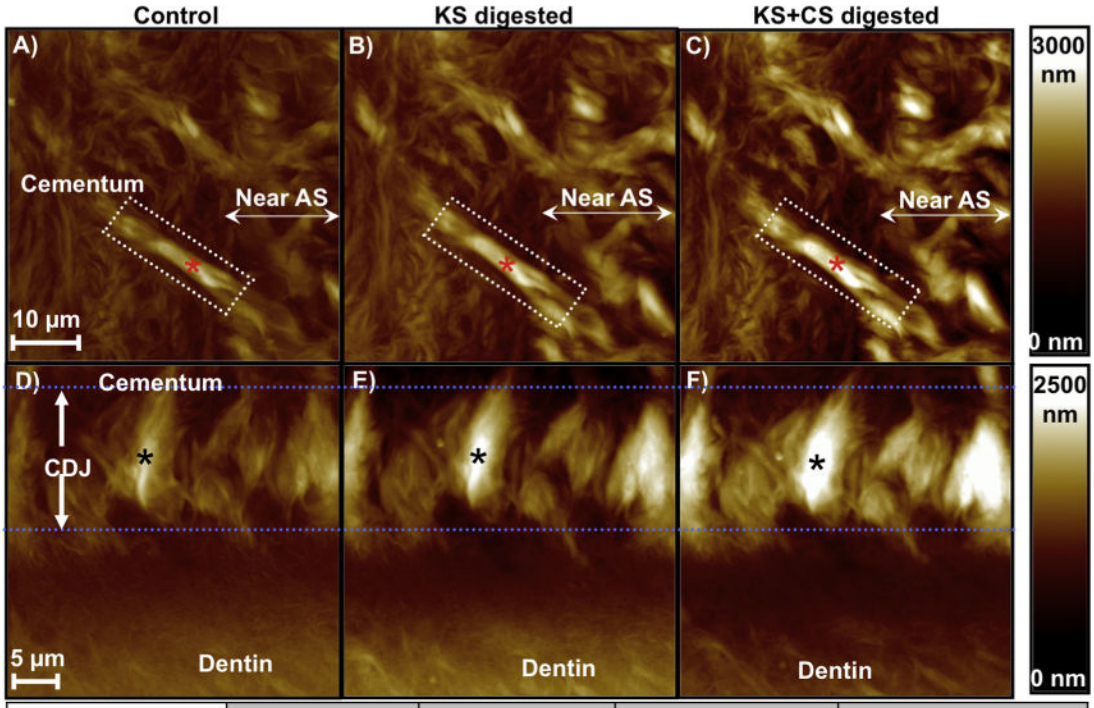

TABLE 1	Tissue type	Control	KS digested	KS + CS digested
Swelling height (nm)	PDL	215 ± 63	280 ± 84	424 ± 94
	PC - CDJ	122 ± 69	160 ± 62	193 ± 79
	SC - CDJ	193 ± 95	283 ± 142	360 ± 159

Fig. 3.

AFM micrographs illustrated a change in swelling characteristics of a single PDL-insert within cementum (A–C, marked by a red asterisk) and in the CDJ (D–F, marked by a black asterisk) following GAG digestion. The intensity scale bars on the right for each row illustrate variation in topographical height. (A, D) exhibited swelling equivalent to undigested conditions, (B, E) post KS-digestion swelling, and (C, F) post KS + CS digestion swelling. The averaged results (Table 1) of PDL-inserts revealed a significant increase in swelling upon GAG digestion (ANOVA tests ($P < 0.05$)). It should be noted that the same PDL–cementum and cementum–dentin interfaces sites were analyzed for each KS and CS digestion condition to accurately monitor the effect of digestion on swelling and mechanical properties. AS: Attachment site.

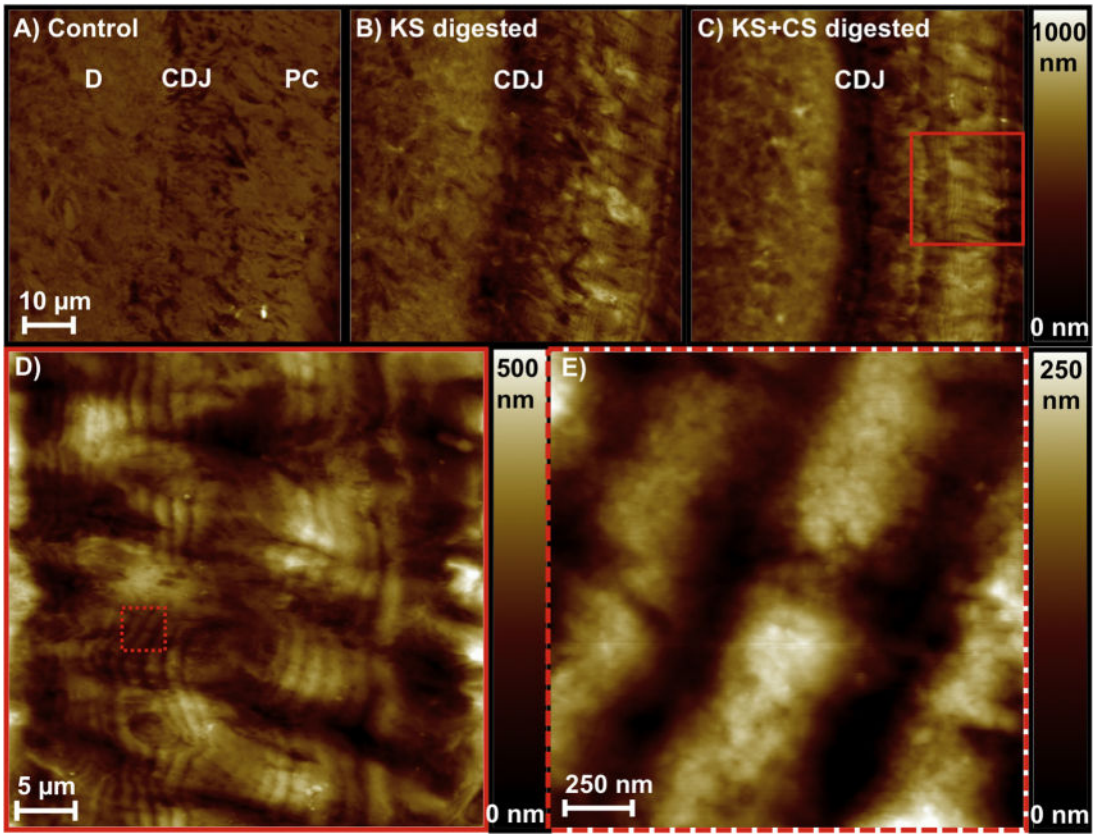

Fig. 4.

AFM micrographs under dry conditions illustrated loss of structural integrity within primary cementum and CDJ through the formation of a valley shown as an increase in depth as the CDJ was depleted of KS (B) and KS + CS GAGs (C) compared to the control (A). Digestion of the polyanionic GAG chains revealed finer lamellar pattern within primary cementum (D, E), and a similar pattern was observed in secondary cementum (not shown).

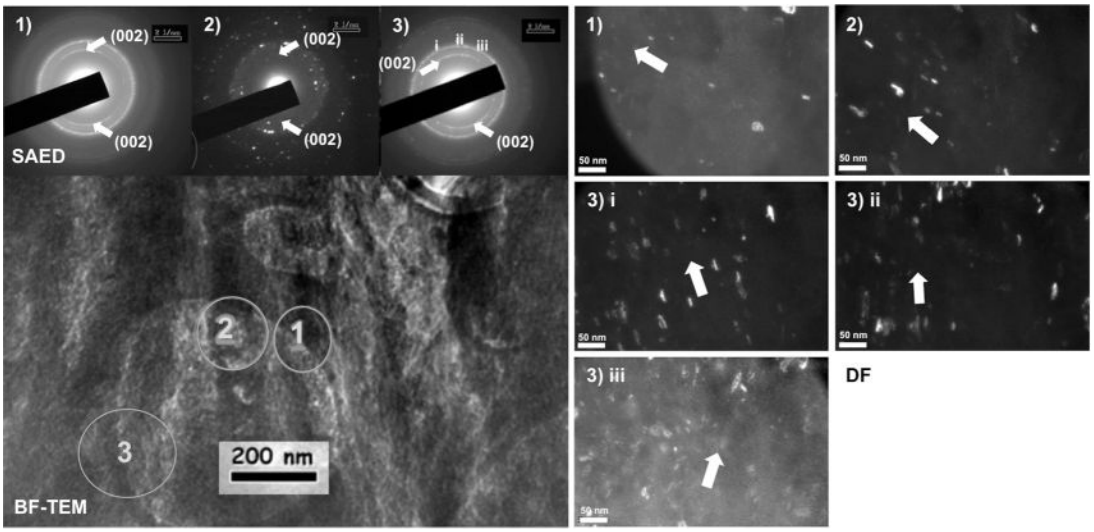

Fig. 5.

Left: bright-field (BF) TEM image with insets of selected area electron diffraction (SAED) patterns at regions marked 1–3. Right: corresponding dark-field (DF) images highlighted the orientation of hydroxyapatite crystals along the 002 *c*-axis, which coincided with collagen fibril direction indicating the presence of intrafibrillar mineral. While crystal orientation maintained a close match to fibril direction, SAED and DF indicated a spread in crystal orientation within the sampled regions and a strong possibility of the presence of extra-fibrillar mineral.

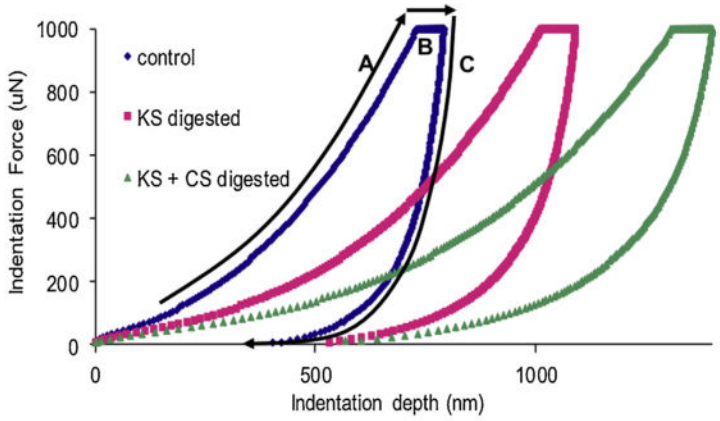

TABLE 2	Tissue type	Control	KS digested	KS + CS digested
Elastic Modulus (GPa)	Enthesis (PDL-Cementum)	1.5 ± 0.7	0.7 ± 0.2	0.4 ± 0.2
	PC - CDJ	2.5 ± 0.7	1.2 ± 0.2	0.8 ± 0.2
	SC - CDJ	2.9 ± 1.3	1.3 ± 0.4	0.7 ± 0.3
	PC - CEM	3.9 ± 1.3	2.2 ± 0.6	1.3 ± 0.2
	SC - CEM	4.2 ± 1.1	2.3 ± 0.6	1.3 ± 0.5
	PC - DEN	17.5 ± 2.9	10.2 ± 2.0	5.6 ± 1.2
	SC - DEN	16.1 ± 3.4	8.2 ± 2.9	4.5 ± 2.0

TABLE 3	Tissue type	Control	KS digested	KS + CS digested
Rate of tissue deformation (nm/sec)	Enthesis (PDL-Cementum)	21 ± 7	37 ± 6	48 ± 22
	PC - CDJ	18 ± 5	24 ± 4	29 ± 6
	SC - CDJ	18 ± 4	24 ± 5	30 ± 6

Fig. 6.

Load-hold-unload segments of the curve for site-specific mechanical testing are shown; loaded to a peak load of 1000 μN—A, 3 s hold of 1000 μN—B, and 3 s unload back to 0 μN—C. Average reduced elastic modulus (Table 2) and the rate of tissue deformation (Table 3) (loss in tissue resilience) results were calculated. Each sequential digestion yielded significant changes in mechanical behavior within the examined tissue type. A subtle variation between PC and SC locations was noted during the predigestion time point and vanished upon KS and CS digestions.